Human-Comfortable Collision Free Navigation for Personal Aerial Vehicles

Nicolas Dousse[1] Grégoire Heitz[1] Felix Schill[2] Dario Floreano[1]

***Abstract*—Semi- or fully-autonomous Personal Aerial Vehicles (PAVs) are currently studied and developed by public and private organizations as a solution for traffic congestion. While optimal collision-free navigation algorithms have been proposed for autonomous robots, trajectories and accelerations for PAVs should also take into account human comfort. In this work, we propose a reactive decentralized collision avoidance strategy that incorporates passenger physiological comfort based on the Optimal Reciprocal Collision Avoidance strategy [1]. We study in simulation the effects of increasing PAV densities on the level of comfort, on the relative flight time and on the number of collisions per flight hour and demonstrate that our strategy reduces collision risk for platforms with limited dynamic range. Finally, we validate our strategy with a swarm of 10 quadcopters flying outdoors.**

***Index Terms*—Aerial Robotics, Collision Avoidance, Intelligent Transportation Systems, Swarms, Distributed Robot Systems.**

I. INTRODUCTION

In many cities, the saturation of the road transportation system and predicted traffic increment [2] demand for innovative alternative solutions. A promising idea for congested cities is the use of the third dimension for personal transportation (Fig. 1). Recently, several projects[1] [3], [4] have investigated the technologies for Personal Aerial Transport Systems (PATS) as breakthrough in 21^{st} century transportation systems.

In a PATS, there could be up to 40 vehicles per cubic kilometer [2] while the densities usually assumed in Air Traffic systems are up to 4 orders of magnitude below [5]. Thus, proposed strategies for air traffic systems (decentralized [6] or centralized [7], [8]) may not be suited at high densities. NASA acknowledges that the current Air Traffic system reaches saturation and would not scale much further. As NASA is expecting that 10 millions vehicles per day will share the US airspace system, they recently launched a Sky for All challenge[2] to find "creative, clean-slate design constructs, or enabling component technologies and concepts, that will inform the design of real-world future air transportation"[3].

Fig. 1. Concept for Personal Aerial Vehicles flying over a city [9].

In dense, highly decentralized and dynamic environments, future PAVs could benefit from autonomous navigation capabilities. Autonomous navigation has received a lot of attention for many years. With state-of-the-art techniques, robots can now autonomously navigate safely in known and partially unknown environments [10], in the presence of other dynamic obstacles or vehicles [11], and even in the presence of humans [12].

In order to be widely accepted as a new mean of transportation, PAVs automation capabilities should not only ensure safety but also tackle the problem of the passengers comfort. Even if some people do appreciate the adrenaline rushes coming from aggressive maneuvers, the vast majority would prefer a quiet ride. If the automation in PAVs cannot guarantee a certain level of comfort, the general public will not adopt this new transportation system [13].

Having comfortable collision-free trajectories is not only important with humans on board but can also deliver some benefits in other situations such as package delivery [14] (the payload can be far from the center of mass and every acceleration provokes additional lever arm to counteract) and fire fighting [15] (water moves back and forth in the tank provoking oscillatory movements that can destabilize the robot.)

Passenger comfort has both a physiological and psychological component [16], but for sake of simplicity in this work we focus on the physiological component.

Some studies about comfort in commercial aviation focus on environmental factors such as in-cabin factors, such as noise, seat size, mobility, cabin pressure and humidity [17]. Other

Manuscript received: May, 30, 2016; Revised September, 20, 2016; Accepted: October, 30, 2016.

This paper was recommended for publication by Editor Nancy Amato upon evaluation of the Associate Editor and Reviewers' comments. This work is part of the myCopter project funded by the European Union under the 7th framework program and by ArmaSuisse, competence sector Science+Technology for the Swiss Federal Department of Defense, Civil Protection and Sport.

[1]N. Dousse, G. Heitz and D. Floreano are with the Laboratory of Intelligent Systems, Ecole Polytechnique Fédérale de Lausanne, 1015 Lausanne, Switzerland. Contact e-mail nicolas.dousse@epfl.ch

[2]F. Schill is with the Distributed Intelligent Systems and Algorithm Laboratory, EPFL, 1015 Lausanne, Switzerland.

Digital Object Identifier (DOI): see top of this page.

[1]http://mycopter.eu/, http://www.pplane-project.org/, http://www.terrafugia.com/, http://www.moller.com/.

[2]http://www.nasa.gov/feature/challenge-is-on-to-design-sky-for-all

[3]https://herox.com/SkyForAll

aviation studies measure the effect of roll oscillation frequency [18], combinations of roll and pitch motion, or combination of roll and vertical oscillations [19], [20] on physiological discomfort. Although these studies have highlighted some of the conditions that lead to discomfort, they do not offer a solution to minimize discomfort.

It has been shown that the level of physiological discomfort for passengers rises with the magnitude of jerk [21], [16], which is the time derivative of acceleration. Previous work on ground vehicles suggested to improve physiological comfort by minimizing the time integral of the square of the jerk in path planning strategies [22], [23]. In addition, patents held by aircraft manufacturer companies have been published, where jerk is used as design criteria to tackle passenger comfort in a path planning strategy in order for aircraft to have a trajectory with constant ground gradient segments [24] or a trajectory following lateral and vertical constraints [25]. However, path planning strategies are only effective as long as vehicles have a global knowledge of their environment or at low density, as they have an exponential complexity in terms of number of vehicles [26]. In a dynamic environment with local and possibly incomplete knowledge, such as in a dense PATS, these approaches could fail to provide safe and comfortable trajectories for each personal aerial vehicle because the situation might change faster than the time needed to obtain global information and to compute a new path. Therefore, it is worth considering the use of reactive collision-avoidance strategies.

Here we propose a method to include physiological comfort in the previously-published Optimal Reciprocal Collision Avoidance (ORCA) strategy [1]. We use simulations of a PATS to show the effects of increasing PAV densities on the level of comfort, on the relative flight time and on the number of collisions and we validate the main results with a group of ten real quadcopters in an outdoor environment.

ORCA has been extended to deal with accelerations limits [27], non-holonomic robots [28] or enforcing C^n continuous control sequences [29]. However, none of these approaches consider the variation of acceleration between consecutive time steps and therefore do not limit the jerk. Alone, these methods would not suffice to maximize passengers comfort and would require some modifications in order to minimize the jerk of the flown trajectories. In this work, we take the original strategy and show how the jerk can be minimized.

The paper is organized as follows: In Section II-A, we summarize the Optimal Reciprocal Collision Avoidance (ORCA) strategy from the literature, then in Section II-B we present our extension of the ORCA strategy to include passenger comfort. In Section III, we apply our strategy in a real-time dynamics simulation to a challenging scenario and discuss the effects of the main parameter and the scalability of our approach. The real-world implementation is presented in Section IV. Finally, in Section V, we give concluding remarks.

II. COMFORTABLE EXTENSION OF ORCA

ORCA is a reactive decentralized collision avoidance strategy that provides sufficient conditions to ensure collision-free navigation of multiple robots [1]. It is based on the Velocity Obstacles paradigm [30]: ORCA is a geometrically based strategy that solves trajectory conflicts in the velocity space.

A. Standard ORCA

It is assumed that all vehicles follow a 3D single-integrator kinematic model (i.e. the control input is directly equal to the velocity of the vehicle[31]) with a maximum speed of v_{max}, that they are using the same strategy and that they can sense the relative position and the relative velocity of their neighbors. At each time step, each vehicle performs a cycle of sensing and acting, ensuring that their trajectory will remain collision free for at least a given amount of time τ.

For a situation with two vehicles A and B, vehicle A computes the Velocity Obstacle set, which is the set of all relative velocities that will lead to a collision between vehicles A and B within a time window τ, noted $VO^{\tau}_{A|B}$. If the relative velocity is outside $VO^{\tau}_{A|B}$, the two vehicles are guaranteed to be collision free for at least τ amount of time (i.e. $\boldsymbol{v}_A - \boldsymbol{v}_B \notin VO^{\tau}_{A|B}$).

If the relative velocity is in $VO^{\tau}_{A|B}$, we define $\boldsymbol{u}$ as the vector from the relative velocity to the closest point outside $VO^{\tau}_{A|B}$. If vehicles A and B alter their relative velocity by at least $\boldsymbol{u}$, they will be collision free for at least a time duration of τ. The way this alteration is done is arbitrary. As vehicles A and B use the same strategy, both vehicles share equally the responsibility to alter their velocity by at least $\frac{1}{2}\boldsymbol{u}$. Therefore, the set of non-colliding velocities for vehicle A with respect to B following this fair shared responsibility is the half-volume pointing in the direction of $\boldsymbol{u}$ at location $\boldsymbol{v}_A^{opt} + \frac{1}{2}\boldsymbol{u}$ and is called $ORCA^{\tau}_{A|B}$.

With more vehicles, this procedure is repeated for each neighboring vehicle. At the end, the set of non-colliding velocities is created by the intersection of all induced half planes.

In a free space without neighboring vehicles, vehicle A would choose $\boldsymbol{v}_A^{pref}$, its preferred velocity. This velocity would typically be given by a higher order planner (e.g. navigation, dynamic path planner). However, in presence of neighbors, choosing $\boldsymbol{v}_A^{pref}$ might lead to a collision. Therefore, once the intersection of planes is created, the new desired velocity, $\boldsymbol{v}_A^{new}$, is the velocity inside this intersection of half planes minimizing the Euclidean distance with $\boldsymbol{v}_A^{pref}$ and is obtained by

$$\boldsymbol{v}_A^{new} = \arg\min \|\boldsymbol{v} - \boldsymbol{v}_A^{pref}\| \text{ with } \boldsymbol{v} \in ORCA^{\tau}_A. \quad (1)$$

B. Comfortable ORCA

We present here below our main contribution in Proposition 1: an extension to ORCA in order to adjust the level of comfort of the passengers.

We work with the following hypothesis. By definition, for the velocity $\boldsymbol{v}(t) \in \mathbb{R}^3$ and the acceleration $\boldsymbol{a}(t) \in \mathbb{R}^3$, minimizing the variation of velocity, $\Delta\boldsymbol{v}(t), \forall t$ implies minimizing the acceleration, $\boldsymbol{a}(t), \forall t$. In addition, for the jerk $\boldsymbol{J}(t) \in \mathbb{R}^3$, minimizing the variation of acceleration, $\Delta\boldsymbol{a}(t), \forall t$ implies minimizing the Jerk $\boldsymbol{J}(t), \forall t$. Thus, a strategy that minimizes

the 3D variation of velocity, $\Delta \boldsymbol{v}(t)$ at every time interval will also minimize the jerk, $\boldsymbol{J}(t)$.

If we take the current velocity of the vehicle as preferred velocity, $\boldsymbol{v}_A^{pref}$ in (1), $\boldsymbol{v}_A^{new}$ will therefore be the minimal change of velocity ensuring a safe trajectory and will thus minimize the jerk of the trajectory. However, even if the vehicle is pointing towards its goal at the beginning, it is not guaranteed that it will reach its goal after an avoidance maneuver, as it will continue in this new direction. Therefore, we formulate the Proposition 1 to overcome this issue. The strategy was developed for 3D environments but can as well be applied in 2D. For ease of visualization, Fig. 2 gives only a 2D graphical interpretation of Proposition 1. In 3D, the intersection of lines defining the collision-free zones becomes an intersection of planes.

Proposition 1. *Let $\boldsymbol{v}_A^{current}$ and $\boldsymbol{v}_A^{pref}$ respectively be the current velocity and the preferred navigation velocity of a vehicle. Let further $ORCA_A^\tau$ be the set obtained from the intersection of half planes following the procedure explained in Section II-A. From (1), we can then obtain $\boldsymbol{v'}_A^{current}$, the new velocity minimizing the change of velocity while ensuring a safe trajectory and $\boldsymbol{v'}_A^{pref}$, the new velocity minimizing the change of preferred navigation velocity while ensuring a safe trajectory.*

We define $\boldsymbol{v}_A^{new}$ as the linear combination of $\boldsymbol{v'}_A^{pref}$ and $\boldsymbol{v'}_A^{current}$:

$$\boldsymbol{v}_A^{new} = (1-\lambda)\cdot \boldsymbol{v'}_A^{pref} + \lambda \cdot \boldsymbol{v'}_A^{current} \text{ with } \lambda \in [0,1). \quad (2)$$

then $\boldsymbol{v}^{new}$ is in $ORCA^\tau$ and therefore is safe.

Proof. From (1), we know that $\boldsymbol{v'}_A^{current}$ and $\boldsymbol{v'}_A^{pref}$ are within $ORCA_A^\tau$ and therefore are collision avoiding velocities. Further, $ORCA_A^\tau$ is convex by construction and (2) holds by definition of a convex set. Therefore, all velocities obtained by (2) are within $ORCA_A^\tau$ and thus are safe. □

The pseudo-code algorithm 1 explain how $\boldsymbol{v}_A^{new}$ is computed for every time step following the procedure of proposition 1.

λ is a parameter allowing to balance between the current velocity and the preferred velocity. On the one hand, the closer λ is to one, the smaller the modification of the current velocity will be and therefore, accordingly the smaller the jerk will be and the trajectory more comfortable. However, the price to pay is a longer trajectory. On the other hand, a λ value close to zero means increasing the modification of the current velocity in order to move more directly towards the vehicle's goal and therefore the jerk will be larger, the flight quicker and the trajectory more direct. Depending on the user's preferences, there is a trade-off to find between comfort and flight time.

Additionally, each vehicle can define its λ by its own and change its value on the go, during a flight, depending on his current preference.

The interval of definition of λ is open at 1 to ensure a convergence toward the goal. Indeed, if λ is equal to one, once the vehicle has performed an avoidance maneuver, it cannot be guaranteed that the vehicle will reach its goal.

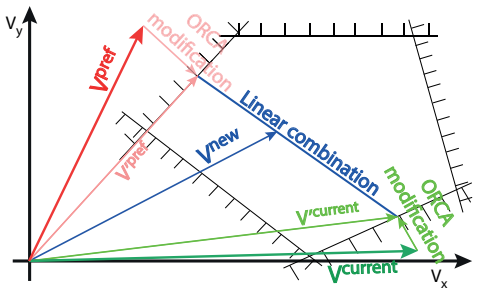

Fig. 2. Visual 2D representation of the Comfortable ORCA strategy. The lines become planes in 3D. $\boldsymbol{v}^{current}$ is the current velocity of the vehicle, $\boldsymbol{v}^{pref}$ is the velocity the vehicle would choose if there were no other vehicles. $\boldsymbol{v'}^{current}$ and $\boldsymbol{v'}^{pref}$ are the velocity obtained by applying (1) on $\boldsymbol{v}^{current}$ and $\boldsymbol{v}^{pref}$ respectively. The new velocity $\boldsymbol{v}^{new}$ is obtained by a linear combination of these two velocities and always lies within $ORCA_A^\tau$.

Algorithm 1 Computation of a new 3D comfortable collision-free velocity

for $i = 1..N_{neighbors}$ **do**
  Sense the relative position and relative velocity of neighbor i.
  Compute the half-volume for neighbor i at location $\boldsymbol{v}_A^{opt} + \frac{1}{2}\boldsymbol{u}_i$, where $\boldsymbol{u}_i \in \mathbb{R}^3$ is defined as in II-A
  Append the half-volume to the $ORCA_A^\tau$ set.
end for
$\boldsymbol{v'}_A^{pref} = \arg\min \|\boldsymbol{v} - \boldsymbol{v}_A^{pref}\|$ with $\boldsymbol{v} \in ORCA_A^\tau$.
$\boldsymbol{v'}_A^{current} = \arg\min \|\boldsymbol{v} - \boldsymbol{v}_A^{current}\|$ with $\boldsymbol{v} \in ORCA_A^\tau$.
$\boldsymbol{v}_A^{new} = (1-\lambda)\cdot \boldsymbol{v'}_A^{pref} + \lambda \cdot \boldsymbol{v'}_A^{current}$.
Send $\boldsymbol{v}_A^{new}$ to the velocity controller.

III. SIMULATION

The extension of ORCA presented in the previous section was implemented in a real-time flight dynamics simulator developed in our laboratory[4]. This simulator, written in ADA, is capable of simulating the dynamics of dynamically constrained flying vehicles in 6 degrees of freedom and runs in discrete time steps. The vehicle dynamics are implemented as a hovering, helicopter-like or multi-rotor-like aircraft, with a body-fixed thrust vector and 3-axis rotational rate control, where accelerations and rates are bounded. Aircraft-specific effects such as rotor dynamics and precise aerodynamics were omitted for simplicity and are not required for this study.

A closed-loop velocity controller allows the vehicles to follow any 3D velocity vector, using a simple yaw coordination controller to align the vehicle with the flight direction. The current vehicle velocity may however deviate from the commanded vector due to the vehicle dynamics constraints. The ORCA implementation was adapted from the C++ RVO2-3D library[5].

The vehicles are represented as a sphere. When two spheres intersect (i.e. the distance between two vehicles is smaller than two times the size of one vehicle), we count this as a collision.

[4]The swarm simulator code is available at https://github.com/lis-epfl/SwarmSimulator.git

[5]The original ORCA C++ code is available at http://gamma.cs.unc.edu/RVO2/.

TABLE I
NUMERICAL VALUES USED IN THE SIMULATIONS

Mass	$100kg$
Distance near miss	$5m$
Distance collision	$3m$
Look-ahead time	$11s$
Circle radius	$798m$
Acceleration limit (on every axis)	$3g$
Cruise speed	$26m/s$ [32]

Implementing a strategy that is planned for single-integrator dynamics on dynamically constrained robots leads to safety violations as ORCA may ask for collision-free velocities that are dynamically not reachable in a single time step. In [29], the authors propose to extend the radius representing the vehicle used in the ORCA strategy to treat a non-holonomic vehicle as holonomic. Similarly, in our work, we extend the radius of the sphere representing the vehicle to encapsulate partially the dynamic constraints of the vehicles. When the distance between two vehicles is smaller than twice this extended radius and larger than twice the size of the vehicle, it is counted as a near miss.

A. Experimental setup

We tested our strategy against the circle scenario in which vehicles travel between two waypoints located on the same altitude at opposite position around the circle. In the scenario's original formulation, the vehicles are starting around the circle, all at the same time. In this situation, all vehicles are perfectly synchronized. This leads to an enormous density at the center of the circle. Even if our strategy can be used in this scenario, as shown with the outdoor experiments in Section IV, in a realistic PATS, the perfect synchronization is highly unlikely and conclusions drawn from this situation would not have practical meaning. To prevent this synchronization, the vehicles start at a uniformly distributed random position inside the circle and then travel back and forth between two waypoints located at opposite side of the circle. This adaptation can model more realistic scenarios than the original formulation. During one experiment, each vehicle is asked to perform 60 crossings of the circle. This corresponds to approximately 1 hour of simulated flight. Each set of parameters is repeated 5 times, each time with different random starting positions and averaged. We compare our results relative to one vehicle flying alone with the same set of parameters and for the same number of crossings.

The set of parameters used in the simulations is defined in Table I.

We then tested our strategy against more complex variations of the circle scenario. First, we added fixed obstacles that can represent for instance tall buildings located at the center of a large city or non-flying zones. Second, we addressed the effects of communication delays by slowing down the update rate of the neighbors position and velocity messages.

Fixed obstacles avoidance was implemented as proposed by [1]. The vehicle adds a new collision avoiding constraint for each static obstacles to the $ORCA^{\tau}_{A}$ set. The vehicle uses the same approach as with neighboring vehicles, except that it takes full responsibility in the avoiding maneuver instead of sharing it. It finally solves (1), as in the case with only neighboring vehicles, with this $ORCA^{\tau}_{A}$ set, composed of fixed obstacles and neighboring vehicles.

B. Results

To address the comfort of the parameter sets, we compute the relative mean total jerk per time unit, $\hat{J}$. It is obtained as follow. The time integral of the square of the jerk, $\boldsymbol{J}i(t)$ is first divided by the travel time, T_{travel} for n vehicles then averaged for every vehicle and for every crossing of the circle. The same ratio is computed for one vehicle flying alone the same number of crossings. We then divide the mean total jerk per time unit for n vehicles by the mean total jerk per time unit for one vehicle and obtain the relative mean total jerk per time unit. Mathematically, the relative mean total jerk per time unit, $\hat{J}$ is obtained by

$$\hat{J} = \frac{\frac{1}{R}\sum_{r=1}^{R}\frac{1}{n}\sum_{i=1}^{n}\frac{\sum_{t=0}^{T_{end}}(\|\boldsymbol{J}_{i_r}(t)\|\Delta t)^2}{T_{travel_{i_r}}}}{\frac{1}{R}\sum_{r=1}^{R}\frac{\sum_{t=0}^{T_{end}}(\|\boldsymbol{J}_{r}(t)\|\Delta t)^2}{T_{travel_{r}}}} \tag{3}$$

where R is the number of repetition of the experiments and T_{end}, the final time of the simulation.

In Fig. 3a, $\hat{J}$ is represented as function of the comfort parameter for different densities. $\hat{J}$ is decreasing with increasing comfort parameter value: the higher the comfort parameter is, the less jerk per time unit the trajectory will have. This result shows that the comfort parameter is capable of decreasing the total jerk and thus increasing the comfort of the trajectory compared to the standard ORCA strategy.

In Fig. 3b, the relative mean travel time is represented as function of the comfort parameter for different densities. The relative travel time is increasing quadratically with the comfort parameter. At high value, once the vehicle has diverged from the path to its goal due to an avoidance maneuver, it takes more time to steer it back on track.

In Fig. 3c, the number of near misses per hour is represented as function of the comfort parameter for different densities. The number of near misses decreases with increasing comfort parameter values. At first, this result is quite surprising. We would expect the opposite as adding this comfort parameter is slowing down the dynamics of the vehicle and thus making it less reactive for avoidance maneuvers. However, according to Proposition 1, the output velocity vector of the Comfortable ORCA strategy is always in the safe set, and limiting the variation in commanded velocity reduces the dynamic requirements from the vehicle. In Fig. 4, the variation of the velocity vector is represented for different comfort parameter values. The smaller the comfort parameter value, the larger the variation of velocity is during one time step. For a dynamically constrained vehicle, this variation may be unfeasible and the actually achieved velocity may lie in the unsafe zone leading to collisions or near-misses. A small velocity variation is more likely to stay in the set of dynamically feasible velocities, and therefore the vehicle's velocity is more likely to remain in the safe set.

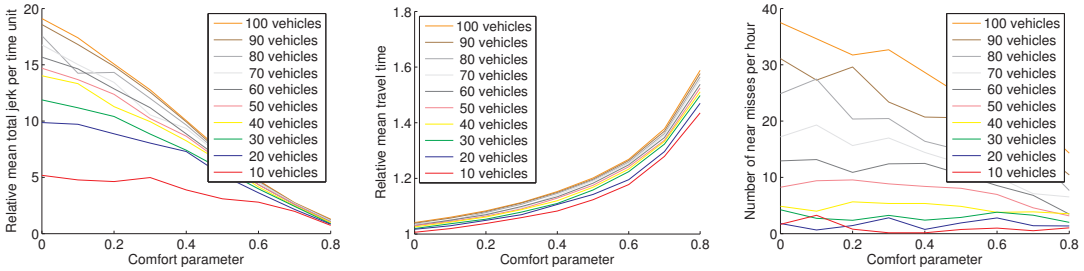

(a) Relative time integral of the square of the jerk per time unit, $\hat{J}$ obtained by (3) as function of the comfort parameter λ.

(b) Relative mean travel time as function of the comfort parameter.

(c) Number of near misses per flight hour as function of the comfort parameter.

Fig. 3. Influence of the comfort parameter λ on the relative mean total jerk, on the relative mean travel time and on the number of near misses per flight hours.

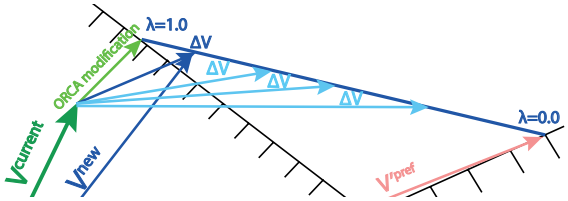

Fig. 4. Euclidean distance between the current velocity, $\boldsymbol{v}^{current}$, and the new velocity, $\boldsymbol{v}^{new}$ depending on the comfort parameter. We can observe that a smaller value for the comfort parameter increases the length of Δv and thus may lead to a velocity that is dynamically unreachable.

Fig. 5. The quadrotors used in the experiments.

C. Additional Results

Results for static obstacles are available in the supplementary materials. The results show a similar trend as for the original case. The relative mean total jerk, $\hat{J}$ is decreased and the relative flight time is increased for λ values getting closer to 1. Fewer near misses were observed for λ values closer to one. Trajectories traces for 10 vehicles and 4 fixed obstacles can be seen the supplementary material. The alteration of the trajectories in order to avoid the fixed obstacles can be clearly seen.

Results for degraded communications are also available in the supplementary materials. The update rate for communication is varied from $0.01s$ up to $0.25s$. Again, the results show a similar trend as for the simpler case. $\hat{J}$ is decreased, the relative flight time is increased and the number of near misses per flight hour still decreases for λ values closer to one with λ getting closer to one, no matter the communication update rate, thus even in presence of degraded communications, our strategy do improve the comfort of the trajectories. Neither $\hat{J}$, nor the relative flight time are influenced by degraded communications. As it could be expected, increasing the time between two messages leads to a higher number of near misses per flight hour. The vehicles are going closer one to each other as they are not aware rapidly enough of the potential threat from a neighbor but are not heavily pushed away from the threat as it could be the case for a potential-based approach.

IV. REAL-WORLD IMPLEMENTATATION

In order to demonstrate the feasibility of this approach under real-time constraints and in real-world conditions, we tested our approach on 10 quadrotors flying outdoors.

A. Flying platform

We designed and built 10 quadrotors to demonstrate our approach in real-world conditions[6]. For experiments with up to ten robots it is important to have a flying robot that is safe to use in large numbers, as well as easy to replicate and repair to be able to maintain a large fleet. All technical details about the design of the robot can be found in our wiki[7].

All computations are done locally on the quadrotor autopilot. The ten quadrotors are fully autonomous: an onboard navigation planner sends 3D velocity commands to drive the robot directly towards its goal. Each robot broadcast periodically its position and velocity while listening to messages incoming from its neighbors. The robots use a time-limited nominal state prediction model [33] to estimate the state of their neighbor between two messages: it is assumed that neighbors continue at the same velocity during a given time window.

ORCA implementation was also adapted from the C++ RVO2-3D library.

B. Experimental setup

The quadrotors take off simultaneously. On action of the operator, all the quadrotors start to cross the circle and move towards their destination located at the opposite point of the

[6]The C code is available at https://github.com/lis-epfl/myCopter.git
[7]http://lis-epfl.github.io/MAVRIC_Library/

circle on the same altitude. ORCA uses the 3D velocity and position extracted from the messages from the neighbors to compute a safe velocity.

The strategy is tested on the original circle scenario previously described, where all vehicles starts to cross the circle at the same time. We used this extreme case of the scenario in order to ensure the safety of the experiments, as it is harder to recognize a failure in 10 Small Drones randomly flying between two waypoints than having them doing one crossing at a time. Each experiment is composed of 5 crossings of the circle. The robots had a cruise speed of 3 m/s.

We compare the experimental results with the same scenario performed in simulation. For the simulation part of this experiment, we modeled the noise of the sensors of the robots. The model of the noise for the position and velocity is similar to the one used by [34]. The accelerometer and velocity measurement errors are modeled by a white Gaussian noise of zero mean. The position measurement error is modeled as a Brownian motion in a parabolic potential centered on the real position of the robot.

C. Results

In this section, we address the effects of the comfort parameter on the relative mean total jerk, $\hat{J}$ on the relative mean travel time and on the number of near misses per flight hour for the circle scenario with 10 quadrotors flying outdoors and compare with the results of the same scenario in simulation.

To address the comfort of the parameter sets, we compute $\hat{J}$ from (3). In Fig. 6a, $\hat{J}$ is represented as function of the comfort parameter. The expected decrease of $\hat{J}$ for increasing comfort parameter value can be observed neither with the outdoor experiment nor in simulation.

Our hypothesis is that the lack of decrease of $\hat{J}$ in Fig. 6a is not coming from real accelerations of the vehicle but rather from measurement noise. To investigate further, we followed two approaches: First, we removed the simulated accelerometer noise from the simulation to compare the results. Second, as post-processing step, we computed the fast Fourier transform (FFT) of the jerk from the real robots to separate flight dynamics from other noise sources such as motor vibrations and sensor noise. Note that the FFT is used only as justification of our method and is not used in the method itself.

We repeated the simulations by computing the jerk with the accelerations without noise. $\hat{J}$ decreases with increasing comfort parameter values (Fig. 8a)) as expected from the simulation results (Fig. 3a). This confirms that the lack of decrease of $\hat{J}$ in Fig. 6a is not coming from real accelerations of the vehicle but rather from measurement noise. The decrease of jerk shown in Fig. 8a is consistent with the previous simulation scenario and validates the use of the comfort parameter in the original circle scenario chosen for the outdoor experiments.

To extract the jerk signal from the noise, we computed the fast Fourier transform (FFT) of the jerk of the recorded data of the outdoor experiments. In Fig. 7, we represent this FFT for the two extreme comfort parameter values of 0 and 0.7 for the Y-axis. Similar results are obtained for the two others axes and for the other comfort parameter values. First, above 1.7 Hz, the amplitudes of the signals are in the same order of magnitude for all comfort parameter values and are likely caused by vibrations and other noise sources. Below 1.7 Hz, the amplitudes of the signal are smaller for the lower comfort parameter than for the higher comfort parameter. We consider the frequency interval of 0.15 Hz to 1.7 Hz. Below 0.15 Hz, the time span of the signal is in the order of magnitude of the time of the experiments (i.e. a crossing of a circle) and it makes no sense to associate these frequencies with a real maneuver. This frequency interval represents the frequency bandwidth in which we are expecting the dynamics of a quadrotor to take place. Additionally, it is also similar to the frequencies at which motion sickness generally happens (below 1 Hz [35]). Therefore a decrease of amplitude in this band can be expected to improve passenger comfort.

In Fig. 8b, we represent the sum of the amplitudes of the jerk FFT divided by the sum of the amplitudes of the jerk for one vehicle flying alone, between 0.15 Hz and 1.7 Hz for different comfort parameter values. The relative sum of jerk amplitudes decreases with increasing comfort parameters for every axis. Thus, the comfort is increased for higher comfort parameter values.

The decrease of the amplitude of the signal at low frequencies as well as the decrease in the relative sum of the amplitudes for increasing comfort parameter values validate again the use of the comfort parameter as tool to increase comfort of the trajectory both in simulation and in outdoor experiments.

In Fig. 6b, the relative mean travel time between two waypoints is represented for the simulation and the real quadrotors. In both cases, the relative flight time increases with the comfort parameter value. This trend was already observed in Fig. 3b. Once the robots performed an avoidance maneuver, it takes more time to steer it back on its path.

In Fig. 6c, the number of near miss per hour is represented as function of the comfort parameter. The number of near misses decreases with increasing comfort parameter similarly to the results obtained in Fig. 3c. The density of this scenario is somehow extreme and even with these near-misses, collisions were never observed during the numerous outdoor flights.

ORCA can vary not only the direction but also the norm of the velocity. During all our tests, the robots velocity varied between 0 m/s (i.e. at some point they had to stop in order to avoid a collision) and 5.5 m/s.

V. CONCLUSIONS AND FUTURE WORKS

We demonstrated a Reactive Comfortable Collision Avoidance strategy that is able to deal with very dense environments. An illustrating video of our simulations and experiments can be seen at https://youtu.be/rrAS2DcOFJU.

Our approach to increase the comfort could also be applied to other version of ORCA. Indeed, our approach remains valid as long as the set of collision-free velocities created by ORCA is convex, which is the case for [27], [28], and [29]. However, the reduction in the number of near misses will probably not be observed anymore as the dynamic limitations of the platform

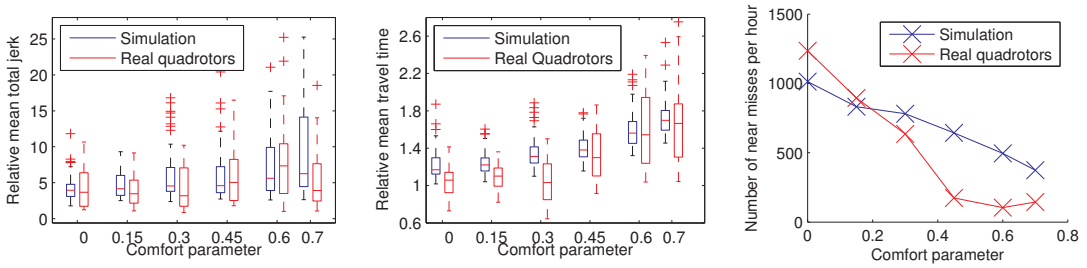

(a) Comparison of relative mean total jerk, $\hat{J}$ obtained by (3).

(b) Comparison of relative travel time.

(c) Comparison of number of near misses per flight hour.

Fig. 6. Comparison of relative mean total jerk $\hat{J}$, relative travel time and number of near misses per flight hour, between outdoor flight experiments and simulations for 10 robots.

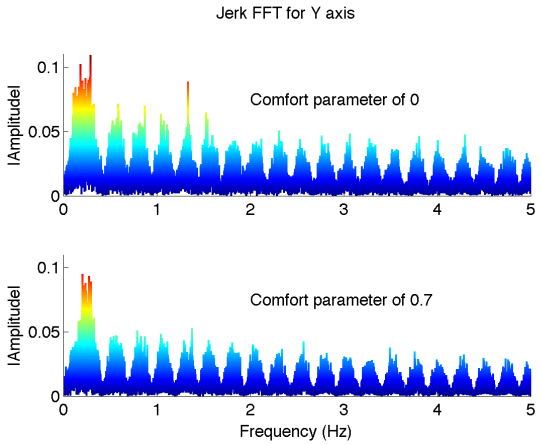

Fig. 7. Jerk FFT for Y-axis for comfort parameter values of 0 and 0.7.

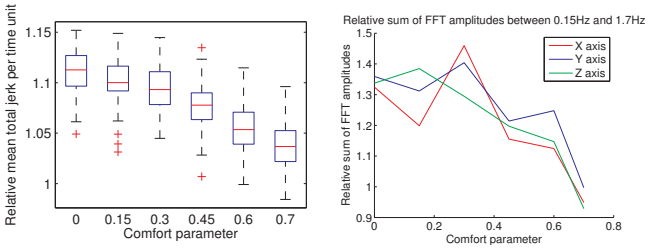

(a) Relative mean total jerk in simulation for the circle scenario with 10 vehicles with jerk computed with accelerometers without noise.

(b) Relative sum of the FFT amplitude for the jerk for all three axis as function of the comfort parameter value.

Fig. 8. Explanation of lack of decrease in relative mean total jerk on Fig. 6a and relative sum of the FFT amplitude proving the decrease in jerk for λ values close to 1.

are already explicitly taken into account in these works. In addition, in order to take into account uncertainties (e.g. noise, inaccurate sensors), the approach of [36] could be used, where the radius of the robots is increased or decreased depending on the sensing uncertainty.

We showed that using the convexity of the collision-free velocities set created following standard ORCA, defining a single parameter was sufficient to increase the comfort of the trajectory as the time integral of the jerk was decreased. We explained the effects of this comfort parameter λ on the relative mean travel time and on the relative mean total jerk per time unit. We also explained why a larger comfort parameter leads to a lower number of near misses. We also applied our strategy to more complex scenario with static obstacles or degraded communication and showed that our approach was also capable of improving passengers comfort in these more realistic situations.

ORCA formulation assumes a synchronous cycle of sensing and acting. We showed that Collision Avoidance is achieved in real-time condition even without enforcing synchronization of sensing and acting cycles. Even in an extremely dense environment and under real-time constraints, collisions never occurred between the real robots.

Our strategy can also fit with user-defined levels of comfort: the comfort parameter λ is not required to be identical for all vehicles and could also change in time. In a realistic scenario, the values for the comfort parameter λ will probably not be equal for every vehicle. Users may prefer shorter and more aggressive trajectories while others may rather fly smoothly at the cost of a longer flight time.

REFERENCES

[1] J. Van Den Berg, S. Guy, M. Lin, and D. Manocha, "Reciprocal n-body collision avoidance," *International Symposium on Robotics Research*, pp. 3–19, 2011.

[2] T. Truman and A. de Graaff, "Out of the box, Ideas about the Future of Air Transport, Part 2," European Commission, Tech. Rep., 2007.

[3] M. Jump, P. Perfect, G. D. Padfield, M. D. White, D. Floreano, P. Fua, J. C. Zufferey, F. Schill, R. Siegwart, and S. Bouabdallah, "myCopter: Enabling Technologies for Personal Air Transport Systems–An Early Progress Report," in *Proceedings of the 37th European Rotorcraft Forum*, 2011, pp. 13–15.

[4] J. M. Hoekstra, "Metropolis WP5 Results and Simulations and Data Analysis," Delft University of Technology, Deliverable D5.2, 2015.

[5] G. Dowek, C. A. Munoz, and V. A. Carreno, "Provably Safe Coordinated Strategy for Distributed Conflict Resolution," in *AIAA Guidance, Navigation, and Control Conference and Exhibit*, San Francisco, California, 2005.

[6] M. Pechoucek and D. Sislak, "Agent-based approach to free-flight planning, control, and simulation," *Intelligent Systems, IEEE*, vol. 24, no. 1, pp. 14–17, 2009.

[7] D. R. Isaacson and H. Erzberger, "Design of a conflict detection algorithm for the Center/TRACON automation system," in *Digital Avionics Systems Conference, 1997. 16th DASC., AIAA/IEEE*, vol. 2, IEEE, 1997, pp. 9–3.

[8] S.-H. Ji, J.-S. Choi, and B.-H. Lee, "A computational interactive approach to multi-agent motion planning," *International Journal of Control Automation and Systems*, vol. 5, no. 3, p. 295, 2007.

[9] A. Cherpillod, "Pendul'Air Design and Realisation of a flying vehicle," Semester Project, EPFL, 2013.

[10] S. Scherer, S. Singh, L. Chamberlain, and M. Elgersma, "Flying Fast and Low Among Obstacles: Methodology and Experiments," *The International Journal of Robotics Research*, vol. 27, no. 5, pp. 549–574, 2008.

[11] P. Nordlund and F. Gustafsson, "Probabilistic Noncooperative Near Mid-Air Collision Avoidance," *Aerospace and Electronic Systems, IEEE Transactions on*, vol. 47, no. 2, pp. 1265 –1276, 2011.

[12] J. Guzzi, A. Giusti, L. M. Gambardella, G. Theraulaz, and G. A. Di Caro, "Human-friendly Robot Navigation in Dynamic Environments," in *Robotics and Automation (ICRA), 2013 IEEE International Conference on*, 2013, pp. 423–430.

[13] B. B. Myers and B. Marshall, "THE INFLUENCE OF COMFORT ON PASSENGER MODAL CHOICE IN WESTERN CANADA," *HUMAN FACTORS IN TRANSPORT RESEARCH EDITED BY DJ OBORNE, JA LEVIS*, vol. 2, 1980.

[14] A.-a. Agha-mohammadi, N. K. Ure, J. P. How, and J. Vian, "Health aware stochastic planning for persistent package delivery missions using quadrotors," in *2014 IEEE/RSJ International Conference on Intelligent Robots and Systems*, IEEE, 2014, pp. 3389–3396.

[15] K. Alexis, G. Nikolakopoulos, A. Tzes, and L. Dritsas, "Coordination of helicopter UAVs for aerial forest-fire surveillance," in *Applications of intelligent control to engineering systems*, Springer, 2009, pp. 169–193.

[16] R. D. Pepler, E. D. Sussman, and L. G. Richards, "PASSENGER COMFORT IN GROUND VEHICLES," *HUMAN FACTORS IN TRANSPORT RESEARCH EDITED BY DJ OBORNE, JA LEVIS*, vol. 2, 1980.

[17] H. Hinninghofen and P. Enck, "Passenger well-being in airplanes," *Autonomic Neuroscience*, vol. 129, no. 1–2, pp. 80–85, 2006.

[18] H. V. C. Howarth and M. J. Griffin, "Effect of Roll Oscillation Frequency on Motion Sickness," *Aviation, Space, and Environmental Medicine*, vol. 74, no. 4, pp. 326–331, 2003.

[19] M. E. McCauley, J. W. Royal, C. D. Wylie, J. F. O'Hanlon, and R. R. Mackie, "Motion sickness incidence: Exploratory studies of habituation, pitch and roll, and the refinement of a mathematical model," DTIC Document, Tech. Rep., 1976.

[20] M. Turner, M. J. Griffin, and I. Holland, "Airsickness and aircraft motion during short-haul flights," eng, *Aviation, space, and environmental medicine*, vol. 71, no. 12, pp. 1181–1189, 2000.

[21] J. Förstberg, "Ride comfort and motion sickness in tilting trains," *TRITA-FKT Report*, vol. 2000, p. 28, 2000.

[22] S. Gulati, C. Jhurani, B. Kuipers, and R. Longoria, "A framework for planning comfortable and customizable motion of an assistive mobile robot," in *Intelligent Robots and Systems (IROS), 2009 IEEE/RSJ International Conference on*, 2009, pp. 4253–4260.

[23] Y. Morales, N. Kallakuri, K. Shinozawa, T. Miyashita, and N. Hagita, "Human-comfortable navigation for an autonomous robotic wheelchair," in *Intelligent Robots and Systems (IROS), 2013 IEEE/RSJ International Conference on*, 2013, pp. 2737–2743.

[24] J. Boyer, R. Auletto, and N. Baloche, "METHOD OF ADAPTING A SEGMENT OF AN AIRCRAFT TRAJECTORY WITH CONSTANT GROUND GRADIENT SEGMENT ACCORDING TO AT LEAST ONE PERFORMANCE CRITERION," pat. US 2016/0085239 A1, Mar. 2016.

[25] M. Le Merrer, B. Dacre-Wright, and F. Coulmeau, "Method of computing aircraft trajectory subject to lateral and vertical constraints," pat. US 2016/0163201, Classification internationale G08G5/00; Classification coopérative G05D1/0005, G08G5/003, G06Q10/047, Mar. 2016.

[26] S. M. LaValle, *Planning algorithms*. Cambridge university press, 2006.

[27] J. van den Berg, J. Snape, S. Guy, and D. Manocha, "Reciprocal collision avoidance with acceleration-velocity obstacles," in *Robotics and Automation (ICRA), 2011 IEEE International Conference on*, 2011, pp. 3475 –3482.

[28] J. Alonso-Mora, A. Breitenmoser, M. Rufli, P. Beardsley, and R. Siegwart, "Optimal Reciprocal Collision Avoidance for Multiple Non-Holonomic Robots," in *Distributed Autonomous Robotic Systems: THE 10th International Symposium*, Berlin, Heidelberg: Springer Berlin Heidelberg, 2013, pp. 203–216.

[29] M. Rufli, J. Alonso-Mora, and R. Siegwart, "Reciprocal Collision Avoidance With Motion Continuity Constraints," *IEEE Transactions on Robotics*, pp. 1–14, 2013.

[30] P. Fiorini and Z. Shiller, "Motion planning in dynamic environments using velocity obstacles," *The International Journal of Robotics Research*, vol. 17, no. 7, pp. 760–772, 1998.

[31] B. Donald, P. Xavier, J. Canny, and J. Reif, "Kinodynamic Motion Planning," *J. ACM*, vol. 40, no. 5, pp. 1048–1066, Nov. 1993.

[32] B. Schuchardt, P. Lehmann, F. Nieuwenhuizen, and P. Perfect, "Deliverable D6.5 Final list of desirable features/ options for the PAV and supporting systems," Tech. Rep., 2015.

[33] J. K Kuchar and L. C Yang, "A review of conflict detection and resolution modeling methods," *Intelligent Transportation Systems, IEEE Transactions on*, vol. 1, no. 4, pp. 179–189, 2000.

[34] C. Virágh, G. Vásárhelyi, N. Tarcai, T. Szörényi, G. Somorjai, T. Nepusz, and T. Vicsek, "Flocking algorithm for autonomous flying robots," *Bioinspiration & Biomimetics*, vol. 9, no. 2, 2014.

[35] A Lawther and M. Griffin, "A survey of the occurrence of motion sickness amongst passengers at sea," *Aviation, space, and environmental medicine*, vol. 59, no. 5, pp. 399–406, 1988.

[36] D. Hennes, D. Claes, W. Meeussen, and K. Tuyls, "Multi-robot collision avoidance with localization uncertainty," in *Proceedings of the 11th International Conference on Autonomous Agents and Multiagent Systems-Volume 1*, International Foundation for Autonomous Agents and Multiagent Systems, 2012, pp. 147–154.